Proceedings of the 8th International Symposium on Cavitation
CAV2012 – Submission No. ##
August 13-16, 2012, Singapore

On the Transition from Sheet to Cloud Cavitation

Thomas Keil
Chair of Fluid Systems Technologies
Technische Universität Darmstadt, Germany

Peter F. Pelz
Chair of Fluid Systems Technologies
Technische Universität Darmstadt, Germany

Johannes Buttenbender
Chair of Fluid Systems Technologies
Technische Universität Darmstadt, Germany

SUMMARY

Hydraulic components failures due to cavitation erosion are mostly a common cause of false or unfavorable operating parameters. In a parameter study with a convergent divergent nozzle, we found a flow change from sheet cavitation to a more aggressive cloud cavitation. This transition occurs at a critical Reynolds number.

The critical Reynolds number was found to be the same for water and a glycol water mixture (increased cinematic viscosity by a factor of 1.16) as one would expect on the grounds of the Bridgman postulate.

The critical Reynolds number, hence the transition point, is predicted by a physical model developed on first principles: The transition point is reached, when the time for sheet growth is the same than the time needed for the reentrant jet to reach the sheet leading edge. If this is the case, the reentrant jets cut of the sheet and detach closed clouds.

To predict the critical Reynolds number is of great value for the industry, since harm full operation points can be identified already in the design process.

INTRODUCTION

Depending on the Reynolds number there are two regimes of cavitation (i) sheet cavitation and (ii) cloud cavitation (see Fig. 1). This could be observed in experiments in a convergent-divergent nozzle test rig [1].

Even though there is a high fluctuation of the trailing edge of the sheet, there is no discrete frequency with that fluctuation and the deformation work done on the surface by sheet cavitation is much smaller in comparison to cloud cavitation.

In the cloud regime, the sheet grows to its maximum length as the cloud moves downstream and collapses. During the sheet growth the kinetic energy of the flow is transferred to the sheet and stored there until the cloud is separated. This energy concentrating process makes cloud cavitation to the most harm full cavitation regime.

For system designer it is useful to know in which regime the cavitation is sheet or cloud cavitation.

The transition point depends on the Reynolds number, the cavitation number and the geometry

$$Re = Re_{crit}(\sigma), \tag{1}$$

$$Re = \frac{\overline{U}H}{\nu}, \tag{2}$$

$$\sigma = \frac{p_A - p_V}{\frac{\rho}{2}\overline{U}^2}, \tag{3}$$

where p_A is the outlet pressure, p_V the vapor pressure, $\overline{U}$ the outlet flow velocity, H the channel height and ν the kinematic viscosity.

For $Re > Re_{crit}$ the clouds separate each cycle time $1/f$. The dimensionless frequency, the Strouhal number depends only on the cavitation number in the cloud regime [1]:

$$St = \frac{fH}{\overline{U}} = St(\sigma). \tag{4}$$

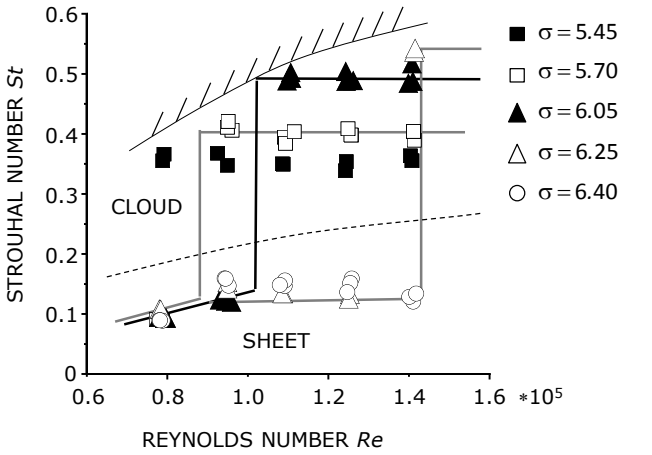

Fig. 1: Transition from sheet to cloud cavitation for the nozzle shape described by Keil, Pelz, Ludwig [1].

Arndt [2] indicates a critical velocity. De Lange [3] observed that for "slow" reentrant jets or "low" angle of attack "viscosity" dominate the cavity behavior. For certain conditions the reentrant jet cannot reach the leading edge of the attached cavity. Up to know no research is known which is first on the grounds of dimensional analysis and second used simple models for the transition from sheet to cloud cavitation. Besides, standard CFD tools such as Fluent or OpenFoam are not able to predict the critical Reynolds number.

In our experiments the main flow is fully turbulent and one might think there should be no Reynolds number effect. This is true for the cloud regime but not for the sheet regime. The friction forces and hence the viscosity is important for the spreading film known as reentrant jet.

Our hypothesis to determine the critical Reynolds number Re_{crit} we observed is the following:

A critical point is reached, when both velocities, first the sheet growth velocity $\overline{U}_S$ and second the spreading velocity of the reentrant jet $\overline{U}_J$ are identical. In contrast, when the reentrant jet (or better viscose spreading film) is slower than the cloud growth, there is no chance to separate "big" clouds which takes all the volume of the attached cavity.

Hence our transition condition is:

$$\begin{aligned} &\text{SHEET REGIME} && \overline{U}_J/\overline{U}_S < 1 \\ &\text{CRITICAL} && (\overline{U}_J/\overline{U}_S)_{crit} = 1 \\ & && \Leftrightarrow Re = Re_{crit}(\sigma) \\ &\text{CLOUD REGIME} && \overline{U}_J/\overline{U}_S > 1\,. \end{aligned} \tag{5}$$

Since the ratio of two velocities is considered, two different models make the critical condition (5). First a model for the sheet growth and second a model for the velocity of the reentrant jet. The viscous friction and hence the Reynolds number comes into play by means of the second model, where the jet is considered to be a viscous spreading film.

The usual name jet for the reentrant jet is misleading, since it suggests a Kirchhoff approach. In fact, many contributions treat the reentrant jets and the sheet by potential flow theory only. Most of them neglect viscous effects between solid walls and the fluid [6]. This approach can lead to some insight for the cloud regime only but not for the transition we focus on.

Krishnaswamy and Andersen [7] also use a potential-theoretic approach to simulate a flow around a profile. They refer to the work of Brewer [8] and [9], who implement a numerical method and solve the boundary layer as well as viscous effects.

EXPERIMENTAL

The nozzle geometry (Fig. 2) is adapted in a close loop test bench. The cross section is rectangular. The narrowest cross height is 2/5 of the channel height. To initiate the sheet cavity an obstacle is placed there. By doing this every side wall friction influences due to surface roughness are small in comparison to the obstacle influence and for this reason not visible in the experiments.

For high-speed visualization the channel consists of acrylic glass and this allows observations from the top and the side view perspective. The velocity of the sheet growth and the movement of the reentrant jet are analyzed with image processing methods. We determine the Strouhal number by image processing. In addition we determine the Strouhal number also by a pressure sensor adapting in the side wall of the channel. Both methods lead to identical results.

We work with two different fluids, water and a water glycol mixture showing an increased kinematic viscosity by a factor of 1.16.

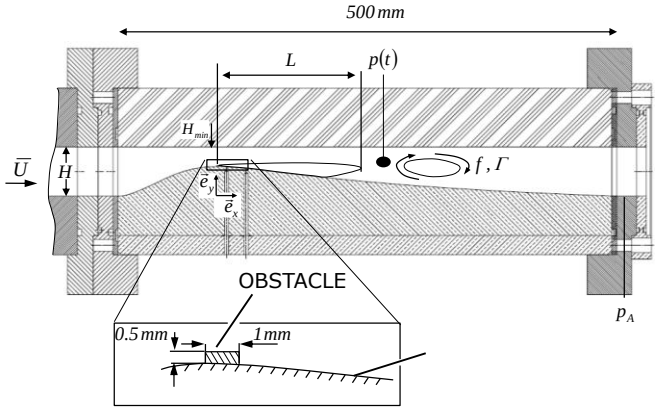

Fig. 2: Nozzle geometry adapted in a close loop test bench at the chair of Fluid Systems Technology - Technische Universität Darmstadt.

OBSERVATIONS

THE STABILITY MAP

As described above, there is a transition from sheet to cloud cavitation when a critical Reynolds number is reached.

In Fig. 3, the Reynolds number is plotted against the cavitation number. The cavitation number ranges from super cavitation to cavitation inception $\sigma_i = 10.5$ for all Reynolds numbers, but excluded from the Fig. 3. The minimum engine speed and the maximum allowable static pressure of test section limit the Reynolds number range.

Filled symbols indicate cloud cavitation regime, unfilled symbols indicate sheet cavitation regime. There is a sharp stability limit given by condition (5), $Re = Re_{crit}(\sigma)$, given by a solid line in the stability map (Fig. 3).

The different marker symbols refer to different viscosities. In the discussion following the presentation of [1], there was an open question if the Reynolds number and cavitation numbers are sufficient to determine the operation point. By our experimental results presented here we indeed showed that there is no direct influence of viscosity but only in form of the Reynolds number. A kinematic viscosity increase of 16% is obtained by a water glycol mixture of approximately 6 vol% glycol. Both liquids show the same transition behavior in the dimensionless form, hence the Bridgman postulate is confirmed also for cavitation.

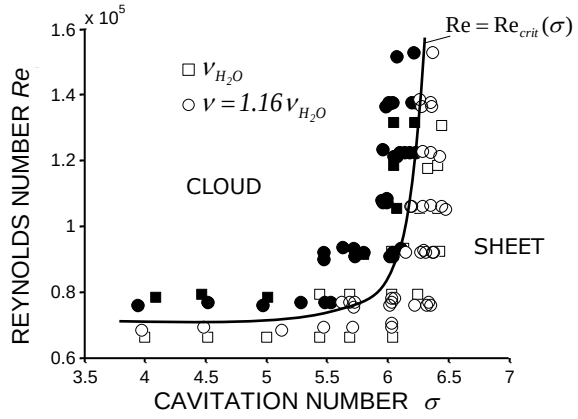

Fig. 3: Stability map: Experimental determined critical Reynolds $Re=Re_{crit}(\sigma)$ number for the transition from sheet to cloud cavitation for two viscosities.

THE CLOUD

A viscose spreading film, called reentrant jet, undermines the sheet. De Lange [3] points out: the formation of the "jet" is responsible for the cloud separation. The separation of the cloud is triggered by that moment, when the spreading film reaches the obstacle at the smallest cross section. In addition the "jet" causes circulation which is imposed to the cloud and finally results in the formation of an U-shaped cavitation vortex [11] and [12]. Buttenbender and Pelz [13] analyzed the effect of stretching and circulation on the dynamic of an U-shaped cavitation vortex modeled as a torus. The basic characteristics of these clouds can be replicated in experiments at the Chair of Fluid Systems Technology.

We observed the following striking phenomena in the cloud regime: The spreading of the film is triggered by the cloud collapse. This is also related to the sudden stoppage of the growing sheet. In other words, the cloud collapse, the stop of the sheet growth and the beginning of the back flowing reentrant jet are nearly simultaneously occurring events which is shown in Fig. 4.

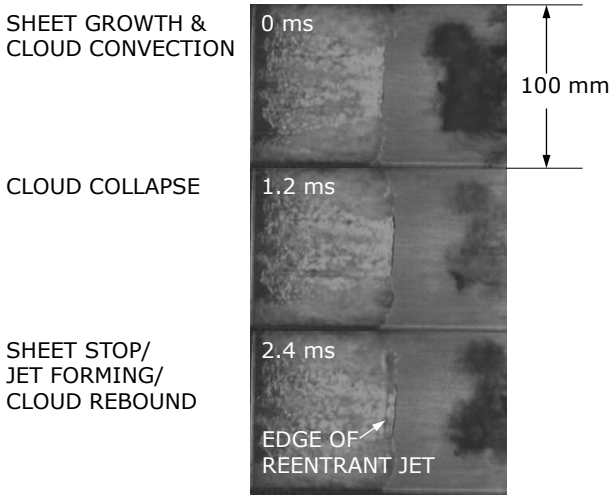

Fig. 4: Forming of the reentrant jet triggered with the cloud collapse operating point for $Re = 110e3$ and $\sigma = 5.4$.

Operating points with sheet dissolved clouds are characterized by a strong periodicity in the separation and the collapse. This periodicity is caused by the sheet growth speed $\overline{U}_S$ and the spreading speed of the viscose film (reentrant jet) $\overline{U}_J$. Both velocities are compared in Fig. 5 in a non-dimensional form for the cloud regime. The bar symbolizes mean quantities in time and space.

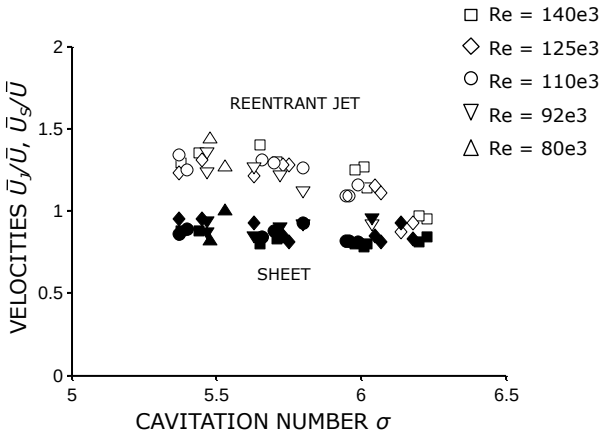

Fig. 5: Velocities of the reentrant jet and the sheet growth for the cloud regime. Note: The velocities are time averaged for the spreading and the sheet growth phase.

The velocity of the mean flow in the smallest cross section is 2.5 times higher than the inlet velocity and thus higher than sheet growth and the jet velocity. Note that the reentrant jet is in the cloud regime up to 1.5 times as fast as the sheet growth velocity. The greater the difference velocities, the more stable the cloud cavitation.

Both velocities increase with decreasing cavitation number. At σ = 6.2 both velocities become similar, which is the critical condition we founded in (5). In fact at that point we observed the transition into sheet cavitation. The next section introduces sheet formed conditions, in which the typical velocity relation is smaller than one.

THE SHEET

We observe the spread of the film (reentrant jet) also in the sheet regime. Fig. 6 shows a corresponding operation point. The arrow marks the edge of the reentrant jet. In comparison to cloud shedding the jet velocity is much smaller in comparison to the sheet growth velocity. We even observe sometimes a stagnation of the jet. The different grey levels between the sheet and the backflow indicate different surface appearance. While the sheet exists of bubble fusion and thus a close cavity with its own surface, the backflow zone exists of many bubbles generated by the shear layer of the jet. Downstream the boundary edge between sheet and jet, the jet cuts of this part of the sheet. Principally, this part may be denoted as cloud nevertheless the operating point is associated with sheet cavitation because of a missing cloud separation. Such zone generally dissolves or recaptured by the faster growing sheet.

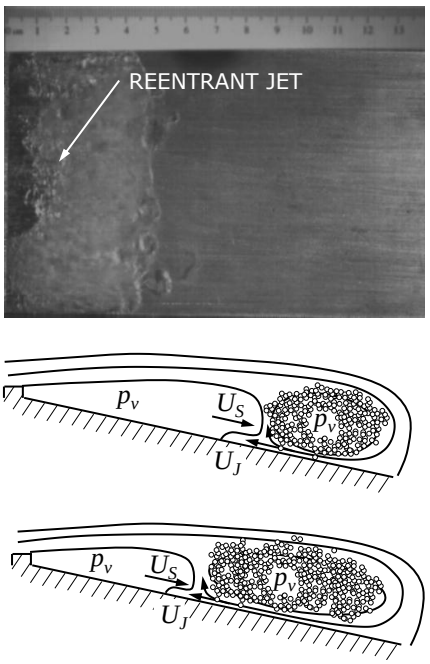

Fig. 6: Reentrant jet for $Re = 75e3$ and $\sigma = 5.7$

The difference of the cloud formation is primary a collapse induced jet in cloud cavitation and a stagnation point induced jet in sheet cavitation. The vapor pressure limits the pressure inside the sheet and inside the vortex part of the sheet.

PHYSICAL MODEL

The critical Reynolds number is determined by the condition (5) given above. Hence we need two physical models, one for the sheet growth and one for the spreading velocity or jet velocity.

ASYMPTOTIC SHEET GROWTH MODEL

Fig. 7 shows schematically our sheet growth model in three steps: first (a: t = 0) the initiation or start of the sheet growth at time equal to zero, second (b: t > 0) the growth of the sheet, and third (c: $t = t_{max}$) the asymptotic stop of the growth.

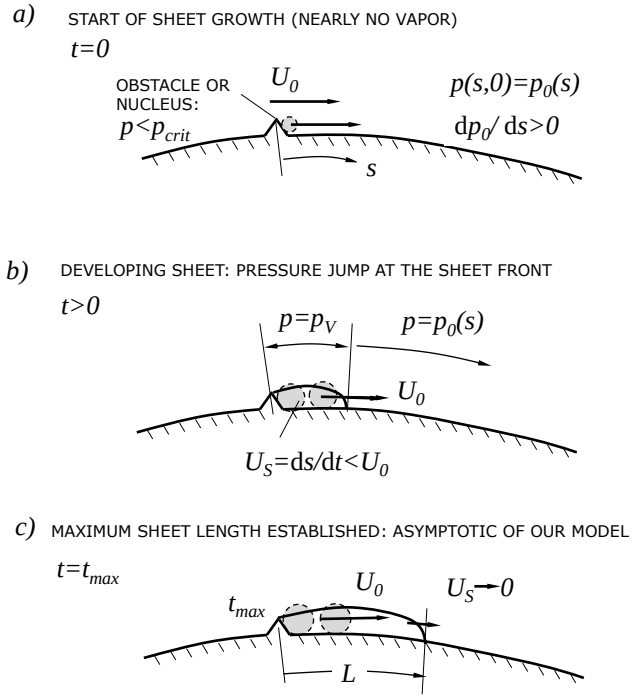

Fig. 7: Asymptotic sheet growth model. a) Growing of a nucleus at s=0, t=0; b). Sheet growth by continuous feeding the sheet by cavitation bubbles traveling with the outer velocity. The bubbles are subjected to the described pressure distribution and follow the RPE. The sheet velocity is smaller than the feed velocity! c) Asymptotically the sheet comes to a rest, as soon as the bubble reaching the sheet front growths unstable.

When a sheet is formed, it is initiated by an obstacle, which is usually a surface roughness of a given geometrical length (in fact, this is confirmed by experiments we did on polished and rough surfaces and will be reported elsewhere). In our model the sheet is feed by bubbles continuously generated at the obstacle and moving downstream with the outer convection velocity U_0. The initial bubble diameter is of the order of the typical obstacle or roughness size. At that point it is important to introduce two necessary conditions for sheet growth we identified:

i. The obstacle size and hence initial bubble is not in equilibrium.
ii. The pressure has to increase downstream of the obstacle to stabilize the sheet (see Fig. 7).

In the growing phase of the sheet all bubbles are subjected to a pressure distribution $p(s)$ along the stream line coordinate s. For $s < 1$ (the actual length of the sheet) the pressure is equal to the vapor pressure. For $s > 1$ we assume the pressure to be equal the initial pressure distribution. This approach is hence a (quite crude) perturbation approach. The bubbles grow following the Rayleigh Plesset Equation (RPE) and the given pressure history described above until they collapse.

Since we model the sheet as a continuous chain of bubbles always the most downstream bubble forms the front of the sheet. When this bubble collapses the next following bubble replaces the leading one.

This approach leads to an asymptotic deceleration of the sheet until the growth comes to rest in the final step (Fig. 7c).

The growth is independent on the Reynolds number but dependents on the cavitation number, since the vapor pressure and the outer pressure are important physical parameters but not the viscosity.

Fig. 8 and Fig. 9 show the comparison of the model (dotted line) with our experimental (filled line) results for a Reynolds number of Re = 140e3 (Fig. 8) and Re = 110e3 (Fig. 9) and two different cavitation numbers. Both curves show the time characteristics of the sheet growth.

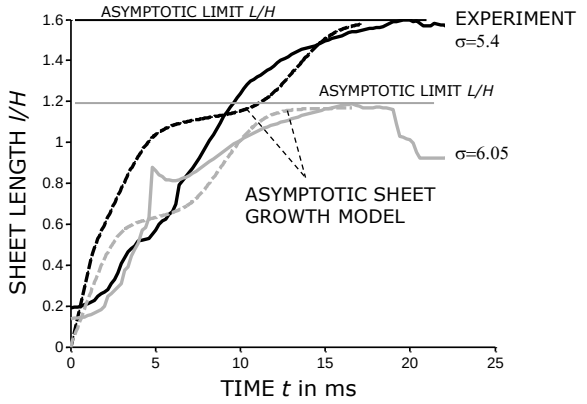

Fig. 8: Comparison of the sheet model and experimental results for Re = 140e3.

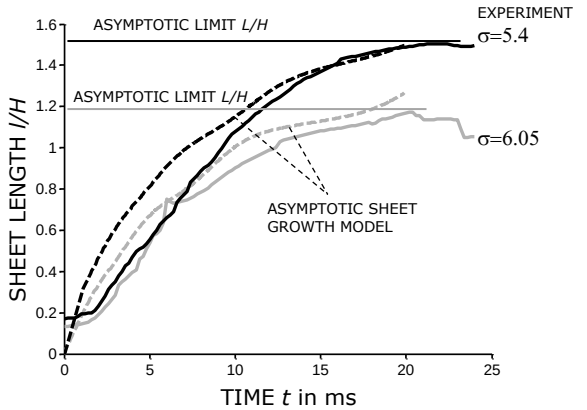

Fig. 9: Comparison of the sheet model and experimental results for Re = 110e3.

The experimental graph is determined with high-speed observations. With image processing we analyzed 17 to 32 different experiments and plotted their mean curve in both figures.

By comparing Fig. 8 and Fig. 9 the difference is small, which confirm the negligible influence of the Reynolds number in this part of the model.

THE REENTRANT JET FILM MODEL

Instead of an often used potential model, we consider the reentrant jet to be a viscous spreading film. To determine the critical condition (5) postulated here for the first time, the friction forces and hence the Reynolds number is essential.

As mentioned above: for the cloud regime the spread of the film is initiated by the cloud collapses. For the more important sheet regime the film growth is triggered by the asymptotic deceleration of the sheet. We first determine the *initial film thickness* by a momentum balance and second use this result to solve the initial value problem for the film spreading.

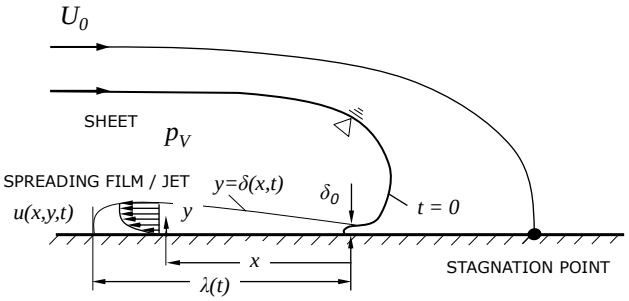

Fig. 10: Reentrant jet considered to be a spreading viscous film.

1. *The Initial Film Thickness*

At $t=0$ (please note we use the same symbol t for both time phases sheet growth and spread of the viscous film) the film starts to form and has its minimal thickness δ_0. At $t=0$ the film velocity is U_0 (see Fig. 10). We determine the initial (and minimal) film thickness δ_0 from the momentum balance in flow direction (see Fig. 11).

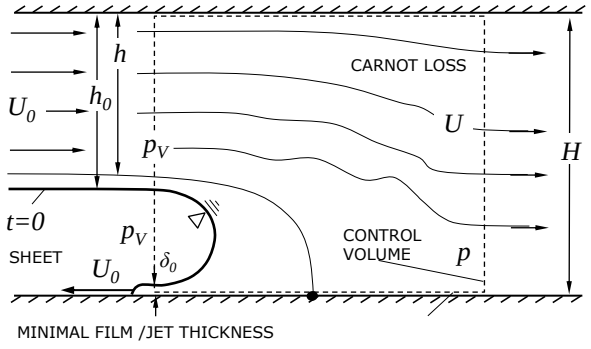

Fig. 11: Control volume for the momentum balance to determine the initial film thickness at $t=0$.

The transient term in the equation of the momentum balance (6) is neglected, which is reasonable at the initial moment when the sheet comes to rest and the film starts growing:

$$-\rho U_0^2 h_0 + \rho U^2 H - \rho U_0^2 \delta_0 = (p_V - p)H. \tag{6}$$

The outlet velocity is determined by the continuity equation:

$$\frac{U}{U_0} = \frac{1}{H}(h_0 - \delta_0). \tag{7}$$

The pressure difference p-p_V is given by the Carnot loss from the cross section h_0 to H, with the discharge coefficient α equal one for the Carnot loss and smaller one for the less dissipative diffusor type flow:

$$\Delta p_{loss} = \alpha \frac{\rho}{2} U_0^2 \left(1 - \frac{U}{U_0}\right)^2 = \alpha \frac{\rho}{2} U_0^2 \left(1 - \frac{h_0}{H}\right)^2. \tag{8}$$

Together with the pressure increase due to the deceleration of the flow the right hand side of the moment balance is given:

$$\frac{p - p_V}{\frac{\rho}{2} U_0^2} = 1 - \left(\frac{U}{U_0}\right)^2 - \frac{\Delta p_{loss}}{\frac{\rho}{2} U_0^2}. \tag{9}$$

In Fig. 5 we saw a decrease of the spread or jet velocity with increasing cavitation number. The cavitation number enters our model by the Equations (6) to (9) since only here the vapor pressure is needed. Hence, the initial film thickness δ_0, which is the initial condition for the spread Equation (17), depends on the cavitation number.

2. The Initial Value Problem for the Film Spreading

In this section we determine the differential equation for the film length λ (see Fig. 10) and the spread or mean jet velocity $U_J = \mathrm{d}\lambda/\mathrm{d}t$. The wall shear stress decelerates the sheet, hence the film thickness $\delta(x)$ will increase along the film according to the continuity equation

$$U_0 \delta_0 = U_J(x)\delta(x). \tag{10}$$

The increase in thickness is sketched in Fig. 10. The velocity distribution within the film is determined by the balance of inertia and viscous forces

$$\frac{\partial u}{\partial t} = \nu \frac{\partial^2 u(y)}{\partial y^2}. \tag{11}$$

As typical for film theory, all changes in spread direction are small in comparison to the other terms in the momentum balance (11) and are hence neglected. Integration of (11) yields the following equation for the mean film (or jet) velocity

$$\frac{dU_J}{dt} = \frac{\nu}{\delta}\left[\frac{\partial u}{\partial y}\right]_0^{\delta}. \tag{12}$$

With the dynamic boundary conditions for the free surface and the wall

$$\left.\frac{\partial u}{\partial y}\right|_{\delta} = 0, \qquad \left.\frac{\partial u}{\partial y}\right|_{0} = -\frac{1}{\mu}\tau_{wall}, \tag{13}$$

the deceleration of the film is given by

$$\frac{dU_J}{dt} = -\frac{\tau_{wall}}{\rho\delta}. \tag{14}$$

We use the boundary layer solution (see Schlichting [15]) for the wall shear stress τ_{wall}

$$\frac{\tau_{wall}}{\rho U_0^2} \sim \frac{1}{\sqrt{Re_J}}. \tag{15}$$

Here the jet Reynolds number depends on the viscosity, the film length λ and the initial jet velocity

$$Re_J = \frac{U_0 \lambda}{\nu}. \tag{16}$$

Using Equations (10), (15) and (16), Equation (17) gives the initial value problem for the film spreading

$$\frac{\ddot{\lambda}}{U_0} + 0.332\sqrt{\frac{\nu}{U_0\lambda}}\,\frac{\dot{\lambda}}{\delta_0} = 0, \qquad \dot{\lambda}(0) = U_0,\ \lambda(0) = 0. \tag{17}$$

The factor 0.332 follows from the boundary layer of a flat plate (see Schlichting [15]). The initial film thickness δ_0 follows from equation (6).

THE TRANSITION

The transition point is given by the critical condition (5): $Re = Re_{crit}(\sigma)$ which was found by [1] but formulated in this form here for the first time (Eqn. (5)). In the stability map (Fig. 3) the transition condition is shown by a solid line.

Our model has two parts, first the asymptotic sheet growth and seconds the initial value problem for the jet spreading. The sheet growth is very good predicted by our model, as can be seen in Fig. 8 and Fig. 9. The jet model exhibits the correct dependence on cavitation number and Reynolds number, although the jet velocity is overvalued for small cavitation numbers. Hence the model correctly predicts the critical condition $\overline{U}_J / \overline{U}_S = 1$. The predicted stability map is shown in Fig. 12 together with the experimental stability limit already seen in Fig. 3. There is a very good agreement between our physical model and the experimental findings.

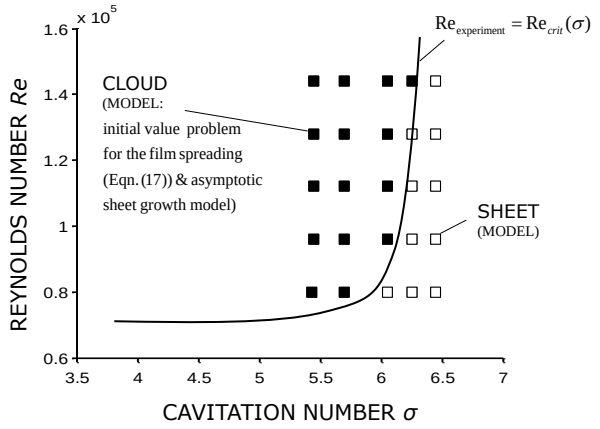

Fig. 12: Predicted stability map & comparison with the experimental stability limit (see Fig. 3 for the experimental results).

DISCUSSION

To predict the transition from sheet to cloud cavitation is of great practical value for the industry. Without a sufficient resolution standard CFD solver are not able to predict that transition as far as we know.

Thus our approach was twofold:

First we did careful experiments on sheet and cloud cavitation. From the experimental observations we formulate a kinematic condition for the transition from sheet to cloud cavitation. We did not consider any phase delay between sheet growth and jet formation. In the past it was an open discussion if or not it is sufficient to give the critical Reynolds number as a function of the cavitation number for the transition. We postulated that the transition condition should be identical independent of the liquid [1]. To confirm this we did experiments with the same Reynolds number but different viscosity and indeed we obtained the very same critical condition. By carefully analyzing our experiments we found that the reentrant jet is triggered by the cloud collapse which might be of interest for the cloud regime. The formation of circulation was discussed in [1] and the consequence of the circulating and stretched cloud is discussed in [13].

Second we developed from first principles two models, one for the sheet growth and one for the reentrant jet.

The two models give some new insights in sheet cavitation and the conditions which have to be full filled. For the sheet growth two conditions have to be fulfilled:

First, the obstacle size is in the same order as the initial bubble size. Second, the pressure has to increase downstream of the obstacle to stabilize the sheet (see Fig. 7). The first condition gives some information about the influence on the role of the surface roughness on sheet cavitation. This gives the motivation for a second stability map separating bubble cavitation from sheet or cloud cavitation. This results will be presented shortly elsewhere. The quite simple sheet model shows an asymptotic behavior, when the sheet comes to rest. It predicts very well the experiments. The second part of our model is the model for the reentrant jet. Since the Reynolds number and hence the viscosity dominate the transition, the jet is treated as a viscous spreading film. The spreading is described by an initial value problem.

The combination of two models enables the prediction of the stability map. The stability limit is very well predicted, the transition point and thus the critical Reynolds number of our model lie in a very good agreement with our experiments.

CONCLUSION

The prediction of the transition from sheet to cloud cavitation is done for the first time. The critical Reynolds number $Re = Re_{crit}(\sigma)$ found in the experiments showed to be the same for different fluids.

With the help of our model we got some important insights into the physics of sheet and cloud cavitation and more over we can supply the industry with a tool to judge the operation point if it is harm full with respect to cavitation erosion or not.

ACKNOWLEDGMENTS

The presented results were obtained within the research project No. 16054 N/1, funded by budget resources of the Bundesministerium für Wirtschaft und Technologie (BMWi) approved by the Arbeitsgemeinschaft industrieller Forschungsvereinigungen “Otto von Guericke” e.V. (AiF).

NOMENCLATURE

SYMBOLS

f	shedding frequency
H	channel height
h	height
L	sheet length
p	pressure
Re	Reynolds number
s	stream line coordinate
St	Strouhal number
t	time
U	velocity
$\overline{U}$	mean velocity
x	coordinate
y	coordinate
α	pressure loss factor
δ	jet/film thickness
λ	film length
μ	dynamic viscosity
ν	kinematic viscosity
ρ	density
σ	cavitation number
τ	shear stress

INDICES

0	initial
A	outlet
crit	critical
J	jet
loss	loss
S	sheet
V	vapor
wall	wall

REFERENCES

[1] Keil, T., Pelz, P.F., Ludwig, G. (2011), *Cloud Cavitation and Cavitation Erosion in Convergent Divergent Nozzle*, WIMRC 3rd International Cavitation Forum, University of Warwick, UK

[2] Arndt, R.E.A., Hambleton, W.T., Kawakami, E. (2009), *Creation and maintenance of cavities under horizontal surfaces in steady and gust flows.* Journal of Fluid Engineering, Nov. 2009, Bde. Vol 131 /111301-1

[3] De Lange, D. F., De Bruin, G. J. (1998), *Sheet cavitation and cloud cavitation, re-entrant jet and three-dimensionality*. Applied Scientific Research, 58(1-4), 91-114

[4] White F. M. (1974), *Viscous Fluid Fow*, McGraw-Hill, ISBN 0-07-069710-8

[5] Homann, F. (1936), *Forsch. Arb. Ing. Wes*., vol. 7 pp 1-10

[6] Cheng, X.-jun; L. C.-jing. (2000), *On the Partially Cavitating Flow Around Two-Dimensional Hydrofoils*. Applied Mathematics and Mechanics, 21(12), 1450-1459.

[7] Krishnaswamy, P., & Andersen, P. (2001), *Re-entrant Jet Modelling for Partially Cavitating Two-Dimensional Hydrofoils*. CAV2001 session B1.005

[8] Brewer, W. (1995), *A Computational and Experimental Study of Viscous Flow Around Cavitationg Propulsors*, Master thesis, Department of Ocean Engineering,

[9] Brewer, W. (1996), *CAV2DBL CAVitating 2-Dimensional with Boundary Layer*, User's manual Version 1.0, Department of Ocean Engineering, MIT

[10] Stutz, B., & Reboud, J.-L. (1997), *Two-Phase Flow Structure of Sheet Cavitation.* Physics of Fluids, 9(12), 3678. doi:10.1063/1.869505

[11] Kawanami, Y., Kato, H., Yamaguchi, H., Maeda, M., Nakasumi, S (2002)., *Inner Structure of Cloud Cavity on a Foil Section*, JSME International Journal, Series B, Vol. 45, No 3

[12] Kawanami, Y., Kato, H., Yamaguchi, H., Tagaya, Y., Tanimura, M. (1997), *Mechanism and Control of Cloud Cavitation*, ASME J. of Fluid Eng., Vol. 119, pp. 788-794

[13] Buttenbender, J., Pelz, P.F. (2012), *The Influence of Imposed Strain Rate and Circulation on Bubble and Cloud Dynamics*, Proceedings of the 8th International Symposium on Cavitation, CAV2012, Singapore

[14] Amromin, E. (2007), *Determination of Cavity Detachment for Sheet Cavitation.* Journal of Fluids Engineering, 129(9), 1105. doi:10.1115/1.2754312

[15] Schlichting, H. (1951), *Grenzschicht-Theorie*, Springer-Verlag, Berlin Heidelberg New York